Efficient calculation of the Coulomb matrix and its expansion around $\mathbf{k} = \mathbf{0}$ within the FLAPW method

Christoph Friedrich [a,*] Arno Schindlmayr [b] Stefan Blügel [a]

[a] *Institut für Festkörperforschung and Institute for Advanced Simulation, Forschungszentrum Jülich, 52425 Jülich, Germany*
[b] *Department Physik, Universität Paderborn, 33095 Paderborn, Germany*

Abstract

We derive formulas for the Coulomb matrix within the full-potential linearized augmented-plane-wave (FLAPW) method. The Coulomb matrix is a central ingredient in implementations of many-body perturbation theory, such as the Hartree-Fock and *GW* approximations for the electronic self-energy or the random-phase approximation for the dielectric function. It is represented in the mixed product basis, which combines numerical muffin-tin functions and interstitial plane waves constructed from products of FLAPW basis functions. The interstitial plane waves are here expanded with the Rayleigh formula. The resulting algorithm is very efficient in terms of both computational cost and accuracy and is superior to an implementation with the Fourier transform of the step function. In order to allow an analytic treatment of the divergence at $\mathbf{k} = \mathbf{0}$ in reciprocal space, we expand the Coulomb matrix analytically around this point without resorting to a projection onto plane waves. Without additional approximations, we then apply a basis transformation that diagonalizes the Coulomb matrix and confines the divergence to a single eigenvalue. At the same time, response matrices like the dielectric function separate into head, wings, and body with the same mathematical properties as in a plane-wave basis. As an illustration we apply the formulas to electron-energy-loss spectra (EELS) for nickel at different $\mathbf{k}$ vectors including $\mathbf{k} = \mathbf{0}$. The convergence of the spectra towards the result at $\mathbf{k} = \mathbf{0}$ is clearly seen. Our all-electron treatment also allows to include transitions from $3s$ and $3p$ core states in the EELS spectrum that give rise to a shallow peak at high energies and lead to good agreement with experiment.

Key words: Coulomb matrix, many-body perturbation theory, dielectric function, electron-energy-loss spectroscopy
PACS: 71.15.Qe, 71.45.Gm

1. Introduction

For the ab initio calculation of electronic excitations and spectroscopic functions, where variational ground-state schemes like Kohn-Sham density-functional theory [1] are not strictly applicable, many-body perturbation theory has now become the method of choice in applications to solids and their surfaces. It is based on a Green-function formalism and an adiabatic switching-on of the Coulomb interaction [2]. In this way the Green function of the fully interacting many-electron system can be expanded in powers of the Coulomb potential, generating a series of Feynman diagrams with increasing complexity. Practical approximations can be designed by terminating the series at a given order or restricting the summation to certain classes

* Corresponding author.
Email address: c.friedrich@fz-juelich.de (Christoph Friedrich).

of self-energy diagrams that describe dominant scattering processes. A prominent example is the exchange-only Hartree-Fock approximation, which includes all electronic interaction effects up to linear order in the Coulomb potential, while additional correlation effects resulting from dynamic screening in an itinerant electron system are taken into account in the GW approximation [3]. The latter has been successfully applied to a variety of materials, especially semiconductors, and generally yields electronic band structures and quasiparticle properties in very good agreement with experimental data [4]. The dielectric function, which already appears as an intermediate quantity in the GW approximation, can be expanded in a similar manner and is itself the key quantity for the theoretical description of optical absorption and related spectroscopies.

For a numerical evaluation of self-energies or dielectric functions in diagrammatic terms it is necessary to project the Coulomb potential, as well as Green functions and all other relevant propagators, onto a suitable basis set. Within the diagrammatic expansion the Coulomb interaction describes the elastic scattering of two electrons or holes, with a possible momentum transfer between initial and final states. The basis for the matrix representation of the Coulomb potential must hence be able to properly describe products of initial-state and final-state wave functions. So far most practical implementations have employed a plane-wave basis set in combination with norm-conserving pseudopotentials. As the product of two plane waves is again a plane wave, this approach has the advantage that products of wave functions can easily be expressed in the same basis as the original wave functions themselves. In addition, fast Fourier transformations may be exploited, and the Coulomb matrix in reciprocal space is known analytically. For semiconductors, in particular, sophisticated theoretical calculations of optical absorption [5] and electron-energy-loss spectra [6], which also include excitonic contributions, have been performed in this way.

While the plane-wave pseudopotential approach works well for sp-bonded semiconductors and simple metals, it becomes inefficient for transition metals and rare earths, where a large number of plane waves are needed to accurately describe the localized d or f orbitals. A similar problem occurs in oxides and other compounds involving first-row elements due to the hard pseudopotentials that only contain minimal screening of the ionic core by the innermost $1s$ electrons. Therefore, these materials are best studied within an all-electron scheme that treats core and valence shells on an equal footing and already incorporates the rapid oscillations of the wave functions close to the nuclei in the basis functions themselves. Here we focus on the full-potential linearized augmented-plane-wave (FLAPW) method [7], which is widely used for electronic-structure calculations of such materials. It divides space into nonoverlapping muffin-tin spheres centered at the atomic positions and into the interstitial region. Inside the muffin-tin spheres the basis functions are constructed from numerical solutions of the radial Schrödinger equation with fixed energy parameters, whose products lie outside the vector space spanned by the original basis functions. Therefore, products of the original basis functions may instead be used to construct a mixed product basis [8], in which the matrix elements of the Coulomb potential with initial and final states are then accurately represented.

While the Coulomb matrix is diagonal in a plane-wave basis and given by a simple analytical expression, its evaluation in the mixed product basis of the FLAPW scheme is much more cumbersome. First, the matrix is no longer diagonal, and all elements must be calculated numerically. This requires an efficient computational procedure. Second, due to the long-range nature of the Coulomb potential $v(r) = 1/r$ in real space, the matrix diverges in the limit of small wave vectors $\mathbf{k} \to \mathbf{0}$. Whereas this divergence is confined to the single head element in the case of a plane-wave basis, all matrix elements now contain divergent terms proportional to $1/k^2$ and $1/k$. Previous all-electron implementations [9,10] of many-body perturbation theory have often bypassed this problem by reverting to a plane-wave basis for the Coulomb potential and related propagators, such as the dielectric function, but the projection leads to a loss of accuracy, because the rapid oscillations of the orbitals close to the atomic nuclei cannot be resolved then. As a consequence, physical effects like core polarization are inadequately described. An alternative approach, the so-called offset-Γ method, employs an auxiliary $\mathbf{k}$-point mesh that is shifted from the origin by a small but finite amount [8,11]. In this way it avoids the singularity, but the use of additional meshes increases the numerical cost; even in the most favorable case, for cubic symmetry, the number of $\mathbf{k}$ points must at least be doubled. Furthermore, the convergence of Brillouin-zone (BZ) integrals involving the Coulomb matrix, for example for the GW self-energy, may be slow with respect to $\mathbf{k}$-point sampling due to the approximate treatment of the quantitatively important region near the zone center.

In this work we derive formulas for the Coulomb matrix in the mixed product basis including its math-

ematically exact expansion around $\mathbf{k} = \mathbf{0}$, which involves terms proportional to $1/k^2$ and $1/k$ as well as constant terms. A proper treatment of the small-wave-vector limit is especially important for the theoretical description of optical spectroscopies with zero momentum transfer, but also for the calculation of the nonlocal Hartree-Fock potential or the GW self-energy, which both involve an integration over the BZ. In a second step, to simplify the numerical treatment we then apply a basis transformation that diagonalizes the Coulomb matrix. This eliminates all $1/k$ terms and again restricts the $1/k^2$ divergence to a single diagonal element, belonging to a constant eigenfunction. The final situation is thus once more analogous to a plane-wave representation, where the dielectric function naturally decomposes into head, wing, and body elements, but we retain the full accuracy of the FLAPW basis set. Furthermore, the present algorithm is very efficient; the computational time for a well-converged Coulomb matrix with 10^5 elements takes less than a second on a modern single-CPU personal computer. The present algorithm is implemented in SPEX [12], a computer code for the calculation of excitation spectra and quasiparticle energies within the GW approximation.

This paper is organized as follows. Section 2 shortly describes the FLAPW method and the mixed product basis used in this work. The formulas for the Coulomb matrix at finite wave vectors are derived in Section 3. We then discuss its expansion around $\mathbf{k} = \mathbf{0}$ and the subsequent diagonalization in Section 4. As a practical illustration, in Section 5 we present electron-energy-loss spectra of Ni calculated at finite $\mathbf{k}$ vectors as well as $\mathbf{k} = \mathbf{0}$ within the random-phase approximation. Finally, Section 6 summarizes our main conclusions. Unless stated otherwise we use Hartree atomic units.

2. Basis sets

2.1. *FLAPW method*

In the FLAPW method space is divided into nonoverlapping atom-centered muffin-tin (MT) spheres and the interstitial region (IR). The core-electron wave functions, which are (mostly) confined to the MT spheres, are directly obtained from a solution of the fully relativistic Dirac equation. The valence-electron wave functions with spin σ are expanded in interstitial plane waves (IPW) in the interstitial region and numerical functions $u^\sigma_{almp}(\mathbf{r}) = u^\sigma_{alp}(r) Y_{lm}(\mathbf{e_r})$ inside the MT sphere of atom a with position vector $\mathbf{R}_a$. The latter comprise solutions of the Kohn-Sham equation

$$\left[-\frac{1}{2}\nabla^2 + \overline{V}^\sigma_{\mathrm{eff},a}(r)\right] u^\sigma_{alm0}(\mathbf{r}) = \epsilon^\sigma_{al} u^\sigma_{alm0}(\mathbf{r}) \tag{1}$$

for $p = 0$ and their first energy derivatives $u^\sigma_{alm1}(\mathbf{r}) = \partial u^\sigma_{alm0}(\mathbf{r})/\partial \epsilon^\sigma_{al}$ for $p = 1$, where $\overline{V}^\sigma_{\mathrm{eff},a}(r)$ is the spherical average of the effective potential, ϵ^σ_{al} are suitably chosen energy parameters, and $Y_{lm}(\mathbf{e_r})$ denote the spherical harmonics. The notation $\mathbf{e_r} = \mathbf{r}/r$ with $r = |\mathbf{r}|$ indicates the unit vector in the direction of $\mathbf{r}$. In a given unit cell the Kohn-Sham wave function at a wave vector $\mathbf{k}$ with band index n and spin σ is then given by

$$\varphi^\sigma_{n\mathbf{k}}(\mathbf{r}) = \begin{cases} \dfrac{1}{\sqrt{N}} \displaystyle\sum_{l=0}^{l_{\max}} \sum_{m=-l}^{l} \sum_{p=0}^{1} A^{n\mathbf{k}\sigma}_{almp} u^\sigma_{almp}(\mathbf{r} - \mathbf{R}_a) & \text{if } \mathbf{r} \in \mathrm{MT}(a) \\ \dfrac{1}{\sqrt{V}} \displaystyle\sum_{|\mathbf{k}+\mathbf{G}| \le G_{\max}} c^{n\mathbf{k}\sigma}_{\mathbf{G}} e^{i(\mathbf{k}+\mathbf{G})\cdot\mathbf{r}} & \text{if } \mathbf{r} \in \mathrm{IR} \end{cases} \tag{2}$$

with the crystal volume V, the number of unit cells N, and cutoff values $l_{\max}$ and $G_{\max}$. The coefficients $A^{n\mathbf{k}\sigma}_{almp}$ are determined by the requirement that the wave function is continuous in value and first radial derivative at the MT sphere boundaries. If desired, additional local orbitals [14] or higher energy derivatives [15] can also be incorporated by allowing $p \ge 2$.

2.2. *Mixed product basis*

The FLAPW method uses continuous basis functions that are defined everywhere in space but have a different mathematical representation in the MT spheres and the IR. For the expansion of wave-function products, however, it is better to employ two separate sets of functions that are defined only in one of the spatial regions and zero in the other. In this way, linear dependences that occur only in one region can easily be eliminated, which overall leads to a smaller and more efficient basis. The resulting combined set of functions is called the mixed product basis.

Inside the MT spheres the mixed product basis must accurately describe the products

$$u^{\sigma\,*}_{almp}(\mathbf{r})u^{\sigma}_{al'm'p'}(\mathbf{r}) = u^{\sigma}_{alp}(r)Y^{*}_{lm}(\mathbf{e_r})u^{\sigma}_{al'p'}(r)Y_{l'm'}(\mathbf{e_r}) = \sum_{L=|l-l'|}^{l+l'}\sum_{M=-L}^{L} C_{lml'm'LM}U^{\sigma}_{aLP}(r)Y_{LM}(\mathbf{e_r})\,, \quad (3)$$

which we expand in spherical harmonics with the Gaunt coefficients

$$C_{lml'm'LM} = \int Y^{*}_{lm}(\mathbf{e_r})Y_{l'm'}(\mathbf{e_r})Y^{*}_{LM}(\mathbf{e_r})\,d\Omega\,. \quad (4)$$

The index P counts the radial product functions $U^{\sigma}_{aLP}(r) = u^{\sigma}_{alp}(r)u^{\sigma}_{al'p'}(r)$ for a given angular quantum number L. We emphasize again that, in general, the latter lie outside the vector space spanned by the original numerical basis functions $\{u^{\sigma}_{almp}(\mathbf{r})\}$. Initially, the set of radial product functions is neither normalized nor orthogonal and usually has a high degree of (near) linear dependence. An effective procedure to remove these (near) linear dependences is to diagonalize the overlap matrix and to retain only those eigenvectors whose eigenvalues exceed a specified threshold value [13]. In this way the MT functions become orthonormalized. By using both spin-up and spin-down products in the construction of the overlap matrix we make the resulting basis spin-independent. If desired, the basis set may be reduced further by introducing an additional cutoff value $L_{\max}$ for the angular quantum number. On the other hand, it must be supplemented with a constant MT function for each atom in the unit cell, which is later needed to represent the eigenfunction that corresponds to the divergent eigenvalue of the Coulomb matrix in the limit $\mathbf{k} \to \mathbf{0}$. From the resulting orthonormal MT functions $M_{aLMP}(\mathbf{r}) = M_{aLP}(r)Y_{LM}(\mathbf{e_r})$ we formally construct Bloch functions

$$M^{\mathbf{k}}_{aLMP}(\mathbf{r}) = \frac{1}{\sqrt{N}}\sum_{\mathbf{T}} e^{i\mathbf{k}\cdot(\mathbf{T}+\mathbf{R}_a)}M_{aLP}(|\mathbf{r}-\mathbf{T}-\mathbf{R}_a|)Y_{LM}(\mathbf{e}_{\mathbf{r}-\mathbf{T}-\mathbf{R}_a})\,. \quad (5)$$

The sum runs over all lattice translation vectors $\mathbf{T}$, and $M_{aLP}(r) = 0$ if r is larger than the muffin-tin radius s_a.

In the IR, since the product of two IPWs equals another IPW, we use the set

$$M^{\mathbf{k}}_{\mathbf{G}}(\mathbf{r}) = \frac{1}{\sqrt{V}}e^{i(\mathbf{k}+\mathbf{G})\cdot\mathbf{r}}\Theta(\mathbf{r}) \quad (6)$$

with the step function

$$\Theta(\mathbf{r}) = \begin{cases} 0 & \text{if } \mathbf{r} \in \text{MT} \\ 1 & \text{if } \mathbf{r} \in \text{IR} \end{cases} \quad (7)$$

and a cutoff $G'_{\max} \le 2G_{\max}$ in reciprocal space. Together with the MT functions we thus obtain the mixed product basis $\left\{M^{\mathbf{k}}_{I}(\mathbf{r})\right\} = \left\{M^{\mathbf{k}}_{aLMP}(\mathbf{r}), M^{\mathbf{k}}_{\mathbf{G}}(\mathbf{r})\right\}$ for the representation of wave-function products. In contrast to the MT functions, which were explicitly orthonormalized, the IPWs are not orthogonal to each other; the elements of their overlap matrix can be calculated analytically and are given by

$$\left\langle M^{\mathbf{k}}_{\mathbf{G}} | M^{\mathbf{k}'}_{\mathbf{G}'}\right\rangle = \delta_{\mathbf{k}\mathbf{k}'}O_{\mathbf{G}\mathbf{G}'}(\mathbf{k}) = \delta_{\mathbf{k}\mathbf{k}'}\Theta_{\mathbf{G}-\mathbf{G}'}\,, \quad (8)$$

where

$$\Theta_{\mathbf{G}} = \frac{1}{V}\int e^{-i\mathbf{G}\cdot\mathbf{r}}\Theta(\mathbf{r})\,d^3r = \begin{cases} 1 - \dfrac{4\pi}{3\Omega}\displaystyle\sum_a s_a^3 & \text{for } \mathbf{G} = \mathbf{0} \\ -\dfrac{4\pi}{\Omega G^3}\displaystyle\sum_a e^{-i\mathbf{G}\cdot\mathbf{R}_a}\left[\sin(Gs_a) - Gs_a\cos(Gs_a)\right] & \text{for } \mathbf{G} \neq \mathbf{0} \end{cases} \quad (9)$$

are the Fourier coefficients of the step function (7) and Ω denotes the unit-cell volume. We also define a second set, the biorthogonal set

$$\tilde{M}_I^{\mathbf{k}}(\mathbf{r}) = \sum_J O_{JI}^{-1}(\mathbf{k}) M_J^{\mathbf{k}}(\mathbf{r}) \tag{10}$$

with the overlap matrix $O_{IJ}(\mathbf{k}) = \langle M_I^{\mathbf{k}} | M_J^{\mathbf{k}} \rangle$. It fulfills the identities

$$\left\langle \tilde{M}_I^{\mathbf{k}} \middle| M_J^{\mathbf{k}} \right\rangle = \left\langle M_I^{\mathbf{k}} \middle| \tilde{M}_J^{\mathbf{k}} \right\rangle = \delta_{IJ} \quad \text{and} \quad \sum_I \left| M_I^{\mathbf{k}} \right\rangle \left\langle \tilde{M}_I^{\mathbf{k}} \right| = \sum_I \left| \tilde{M}_I^{\mathbf{k}} \right\rangle \left\langle M_I^{\mathbf{k}} \right| = 1 \,, \tag{11}$$

where the completeness relation is only valid in the subspace spanned by the mixed product basis, however. As the MT functions and the IPWs are defined in different regions of space and the MT functions are orthonormal, only the IPWs overlap in a nontrivial way. It should be noted that the overlap matrix is $\mathbf{k}$-dependent because the size of the mixed product basis varies for different $\mathbf{k}$ vectors.

For the evaluation of the Coulomb matrix elements we have to find a numerically tractable expression for the IPWs. A straightforward approach might employ the Fourier transform of the step function and rewrite (6) as a sum over reciprocal lattice vectors

$$M_{\mathbf{G}}^{\mathbf{k}}(\mathbf{r}) = \lim_{G_{\mathrm{PW}} \to \infty} \frac{1}{\sqrt{V}} \sum_{|\mathbf{G}'| \leq G_{\mathrm{PW}}} \Theta_{\mathbf{G}'} e^{i(\mathbf{k}+\mathbf{G}+\mathbf{G}')\cdot\mathbf{r}} \,, \tag{12}$$

where G_{PW} is a cutoff radius in reciprocal space, for which we must of course choose a finite value in practice. Eq. (12) has a very simple mathematical structure and is easy to implement. For example, the calculation of the matrix elements IPW-IPW only involves Fourier coefficients of the step function $\Theta(\mathbf{r})$ and the Coulomb interaction $1/r$, which are both known analytically. As an alternative, we may exploit the Rayleigh expansion

$$e^{i\mathbf{k}\cdot\mathbf{r}} = \sum_{l=0}^{\infty} 4\pi i^l j_l(kr) \sum_{m=-l}^{l} Y_{lm}^*(\mathbf{e}_{\mathbf{k}}) Y_{lm}(\mathbf{e}_{\mathbf{r}}) \tag{13}$$

involving the spherical Bessel functions $j_l(x)$ in order to subtract the plane waves inside the MT spheres

$$M_{\mathbf{G}}^{\mathbf{k}}(\mathbf{r}) = \lim_{l_{\mathrm{PW}} \to \infty} \frac{1}{\sqrt{V}} \left[e^{i\mathbf{q}\cdot\mathbf{r}} - 4\pi \sum_{\mathbf{T}} \sum_a e^{i\mathbf{q}\cdot(\mathbf{T}+\mathbf{R}_a)} \theta(s_a - r') \sum_{l=0}^{l_{\mathrm{PW}}} i^l j_l(qr') \sum_{m=-l}^{l} Y_{lm}^*(\mathbf{e}_{\mathbf{q}}) Y_{lm}(\mathbf{e}_{\mathbf{r}'}) \right] , \tag{14}$$

where we use the abbreviations $\mathbf{q} = \mathbf{k} + \mathbf{G}$ and $\mathbf{r}' = \mathbf{r} - \mathbf{T} - \mathbf{R}_a$, and $\theta(r)$ denotes the Heaviside function. In a practical implementation we must use a finite maximal angular momentum l_{PW}, which thus becomes the relevant convergence parameter. Despite its more complicated mathematical appearance, we have found that this representation in fact facilitates a considerably faster numerical evaluation because of the slow convergence of the step function in (12) with respect to the number of Fourier coefficients. We illustrate this point in Section 5. In our subsequent derivation we hence employ expression (14).

3. Coulomb matrix at finite k

In this section we derive the formulas for the computation of the Coulomb matrix elements

$$v_{IJ}(\mathbf{k}) = \iint \frac{M_I^{\mathbf{k}*}(\mathbf{r}) M_J^{\mathbf{k}}(\mathbf{r}')}{|\mathbf{r} - \mathbf{r}'|} \, d^3r \, d^3r' \tag{15}$$

for arbitrary finite wave vectors; the limit $\mathbf{k} \to \mathbf{0}$ is discussed in Section 4. Due to the composite basis set $\left\{ M_I^{\mathbf{k}}(\mathbf{r}) \right\}$, which consists of MT functions with $I = (aLMP)$ and IPWs with $I = \mathbf{G}$, the Coulomb matrix is made of four distinct blocks. As it is Hermitian, however, the two off-diagonal blocks are complex conjugates of each other, and thus we have to consider only three blocks explicitly, which correspond to the combinations MT-MT, MT-IPW, and IPW-IPW. Svane and Andersen [16] already examined the matrix elements MT-MT for finite $\mathbf{k}$ vectors in the context of the linearized muffin-tin orbital (LMTO) method. In the following we summarize the derivation in a somewhat different notation and then give the expressions for the additional matrix elements involving IPWs.

3.1. *MT-MT*

If we insert the Bloch representation (5) for the MT functions in

$$v_{aLMP,a'L'M'P'}(\mathbf{k}) = \iint \frac{M^{\mathbf{k}\,*}_{aLMP}(\mathbf{r}) M^{\mathbf{k}}_{a'L'M'P'}(\mathbf{r}')}{|\mathbf{r}-\mathbf{r}'|}\, d^3r\, d^3r'\,, \tag{16}$$

then the integral can be rewritten as

$$\begin{aligned} v_{aLMP,a'L'M'P'}(\mathbf{k}) &= \sum_{\mathbf{T}} e^{i\mathbf{k}\cdot(\mathbf{T}+\mathbf{R}_{aa'})} \\ &\times \iint \frac{M_{aLP}(r) Y^*_{LM}(\mathbf{e}_\mathbf{r}) M_{a'L'P'}(|\mathbf{r}'-\mathbf{T}-\mathbf{R}_{aa'}|) Y_{L'M'}(\mathbf{e}_{\mathbf{r}'-\mathbf{T}-\mathbf{R}_{aa'}})}{|\mathbf{r}-\mathbf{r}'|}\, d^3r\, d^3r'\,, \end{aligned} \tag{17}$$

where the difference vector $\mathbf{R}_{aa'} = \mathbf{R}_{a'} - \mathbf{R}_a$ points from one MT center to another in the same unit cell. The integrals in (17) corresponding to $\mathbf{R} = \mathbf{0}$ and $\mathbf{R} \neq \mathbf{0}$ with $\mathbf{R} = \mathbf{T} + \mathbf{R}_{aa'}$ give rise to two contributions

$$v_{aLMP,a'L'M'P'}(\mathbf{k}) = \delta_{aa'} v^{(\mathrm{a})}_{aLMP,aL'M'P'} + v^{(\mathrm{b})}_{aLMP,a'L'M'P'}(\mathbf{k})\,, \tag{18}$$

which we evaluate separately in the following.

Let us first consider the integral for $\mathbf{R} = \mathbf{0}$. It can be simplified considerably by inserting the identity

$$\frac{1}{|\mathbf{r}-\mathbf{r}'|} = \sum_{l=0}^{\infty} \frac{4\pi}{2l+1} \frac{r_<^l}{r_>^{l+1}} \sum_{m=-l}^{l} Y_{lm}(\mathbf{e}_\mathbf{r}) Y^*_{lm}(\mathbf{e}_{\mathbf{r}'})\,, \tag{19}$$

where $r_<$ and $r_>$ indicate the smaller and larger value of $\{r, r'\}$, respectively. After carrying out the angular integrations we obtain

$$\begin{aligned} &v^{(\mathrm{a})}_{aLMP,aL'M'P'} \\ &= \delta_{LL'}\delta_{MM'} \frac{4\pi}{2L+1} \int_0^{s_a} M_{aLP}(r) \left[\frac{1}{r^{L-1}} \int_0^r r'^{L+2} M_{aLP'}(r')\, dr' + r^{L+2} \int_r^{s_a} \frac{M_{aLP'}(r')}{r'^{L-1}}\, dr' \right] dr\,. \end{aligned} \tag{20}$$

The remaining integrations can be easily performed by standard numerical techniques on a radial mesh.

For the integrals with $\mathbf{R} \neq \mathbf{0}$ we may formally define a multipole potential

$$\Phi(\mathbf{r}) = \int \frac{M_{a'L'P'}(|\mathbf{r}'-\mathbf{R}|) Y_{L'M'}(\mathbf{e}_{\mathbf{r}'-\mathbf{R}})}{|\mathbf{r}-\mathbf{r}'|} d^3r' = \frac{4\pi}{2L'+1} \frac{Q_{a'L'P'}}{|\mathbf{r}-\mathbf{R}|^{L'+1}} Y_{L'M'}(\mathbf{e}_{\mathbf{r}-\mathbf{R}}) \tag{21}$$

that acts in the first MT sphere as a result of a "charge distribution" $M_{a'L'M'P'}(\mathbf{r}'-\mathbf{R})$ in the second, where $Q_{a'L'P'}$ denotes the multipole moments

$$Q_{a'L'P'} = \int_0^{s_{a'}} r'^{L'+2} M_{a'L'P'}(r')\, dr'\,. \tag{22}$$

Using the expansion theorem [17,18]

$$\frac{4\pi}{2L'+1} \frac{1}{|\mathbf{r}-\mathbf{R}|^{L'+1}} Y_{L'M'}(\mathbf{e}_{\mathbf{r}-\mathbf{R}}) = (-1)^{L'+M'} \sum_{l=0}^{\infty} \sum_{m=-l}^{l} c_{L'M',lm} \frac{r^l}{R^{L'+l+1}} Y_{lm}(\mathbf{e}_\mathbf{r}) Y^*_{(L'+l)(m-M')}(\mathbf{e}_\mathbf{R}) \tag{23}$$

with the symmetric matrix

$$\begin{aligned} c_{L'M',lm} &= (-1)^{M'} (4\pi)^2 \frac{[2(L'+l)-1]!!}{(2L'+1)!!(2l+1)!!} C_{L'M'lm(L'+l)(m-M')} \\ &= (4\pi)^{3/2} \frac{1}{\sqrt{(2L'+1)(2l+1)\,[2(L'+l)+1]}} \sqrt{\frac{(L'+l+m-M')!(L'+l-m+M')!}{(L'+M')!(L'-M')!(l+m)!(l-m)!}}\,, \end{aligned} \tag{24}$$

the multipole potential (21) created by a MT function at $\mathbf{R}$ can then be written in terms of radial functions and spherical harmonics at the origin. The corresponding "electrostatic interaction energy" is given by

$$\iint \frac{M_{aLP}(r)Y^*_{LM}(\mathbf{e}_\mathbf{r})M_{a'L'P'}(|\mathbf{r}'-\mathbf{R}|)Y_{L'M'}(\mathbf{e}_{\mathbf{r}'-\mathbf{R}})}{|\mathbf{r}-\mathbf{r}'|}\,d^3r\,d^3r'$$
$$= (-1)^{L'+M'}c_{L'M',LM}Q_{aLP}Q_{a'L'P'}\frac{1}{R^{L+L'+1}}Y^*_{(L+L')(M-M')}(\mathbf{e}_\mathbf{R})\,. \tag{25}$$

After performing the sum over lattice vectors in (17) we eventually obtain

$$v^{(\mathrm{b})}_{aLMP,a'L'M'P'}(\mathbf{k}) = (-1)^{L'+M'}e^{i\mathbf{k}\cdot\mathbf{R}_{aa'}}c_{L'M',LM}Q_{a'L'P'}Q_{aLP}S^{aa'}_{(L+L')(M-M')}(\mathbf{k}) \tag{26}$$

with

$$S^{aa'}_{lm}(\mathbf{k}) = \sum_{\mathbf{T}} e^{i\mathbf{k}\cdot\mathbf{T}}\frac{1}{|\mathbf{T}+\mathbf{R}_{aa'}|^{l+1}}Y^*_{lm}(\mathbf{e}_{\mathbf{T}+\mathbf{R}_{aa'}})\,, \tag{27}$$

where the sum runs over all lattice vectors excluding the case $\mathbf{T}+\mathbf{R}_{aa'}=\mathbf{0}$. We note that $S^{aa'}_{lm}(\mathbf{k})$ is closely related to the structure constant defined in the context of the LMTO method [17]; however, it is not dimensionless and therefore *not* a constant of a given crystal structure. For the numerical evaluation of $S^{aa'}_{lm}(\mathbf{k})$ one must apply the Ewald summation technique.

3.2. *MT-IPW*

For the matrix elements in the off-diagonal block

$$v_{aLMP,\mathbf{G}}(\mathbf{k}) = \iint \frac{M^{\mathbf{k}\,*}_{aLMP}(\mathbf{r})M^{\mathbf{k}}_{\mathbf{G}}(\mathbf{r}')}{|\mathbf{r}-\mathbf{r}'|}\,d^3r\,d^3r' \tag{28}$$

we can again introduce a formal "charge distribution" given by $M^{\mathbf{k}}_{\mathbf{G}}(\mathbf{r}')$ that creates a potential

$$\Phi(\mathbf{r}) = \int \frac{M^{\mathbf{k}}_{\mathbf{G}}(\mathbf{r}')}{|\mathbf{r}-\mathbf{r}'|}\,d^3r' = \frac{1}{\sqrt{V}}\left(4\pi\frac{e^{i(\mathbf{k}+\mathbf{G})\cdot\mathbf{r}}}{|\mathbf{k}+\mathbf{G}|^2} - \int_{\mathrm{MT}}\frac{e^{i(\mathbf{k}+\mathbf{G})\cdot\mathbf{r}'}}{|\mathbf{r}-\mathbf{r}'|}\,d^3r'\right), \tag{29}$$

where the integral runs over the combined volume of all MT spheres, cutting out the plane waves inside them. The "electrostatic interaction energy" arising from the first term in the brackets is given by

$$\frac{4\pi}{\sqrt{V}}\frac{1}{q^2}\int M^{\mathbf{k}\,*}_{aLMP}(\mathbf{r})e^{i\mathbf{q}\cdot\mathbf{r}}d^3r = \frac{(4\pi)^2 i^L}{\sqrt{\Omega}}Y^*_{LM}(\mathbf{e}_\mathbf{q})e^{i\mathbf{G}\cdot\mathbf{R}_a}\frac{1}{q^2}\int_0^{s_a} r^2 M_{aLP}(r)j_L(qr)\,dr\,, \tag{30}$$

where we have again used the Rayleigh expansion (13) and the abbreviation $\mathbf{q}=\mathbf{k}+\mathbf{G}$. If the exponential function in the second term on the right-hand side of (29) is also replaced by the Rayleigh expansion, then the resulting integrals are equivalent to those considered in Section 3.1 above. We can hence evaluate them in the same way. The resulting final expression for the Coulomb matrix element

$$v_{aLMP,\mathbf{G}}(\mathbf{k}) = v^{(\mathrm{a})}_{aLMP,\mathbf{G}}(\mathbf{k}) + v^{(\mathrm{b})}_{aLMP,\mathbf{G}}(\mathbf{k}) + v^{(\mathrm{c})}_{aLMP,\mathbf{G}}(\mathbf{k}) \tag{31}$$

consists of three distinct terms, which are given by

$$v^{(\mathrm{a})}_{aLMP,\mathbf{G}}(\mathbf{k}) = \frac{1}{\sqrt{\Omega}}(4\pi)^2 i^L Y^*_{LM}(\mathbf{e}_\mathbf{q})e^{i\mathbf{G}\cdot\mathbf{R}_a}\frac{1}{q^2}\int_0^{s_a} r^2 M_{aLP}(r)j_L(qr)\,dr\,, \tag{32a}$$

$$v^{(\mathrm{b})}_{aLMP,\mathbf{G}}(\mathbf{k}) = -\frac{1}{\sqrt{\Omega}}(4\pi)^2 i^L Y^*_{LM}(\mathbf{e}_\mathbf{q})e^{i\mathbf{G}\cdot\mathbf{R}_a}\frac{1}{2L+1}\int_0^{s_a} M_{aLP}(r)\left[\frac{\mathcal{I}_L(q,r)}{r^{L-1}} + r^{L+2}\mathcal{J}_{aL}(q,r)\right]dr\,, \tag{32b}$$

$$v^{(\mathrm{c})}_{aLMP,\mathbf{G}}(\mathbf{k}) = -\frac{1}{\sqrt{\Omega}}e^{-i\mathbf{k}\cdot\mathbf{R}_a}Q_{aLP}\sum_{l'=0}^{l_{\mathrm{PW}}}\sum_{m'=-l}^{l}(-1)^{l'+m'}\sum_{a'}e^{i\mathbf{q}\cdot\mathbf{R}_{a'}}c_{Ll'm',LM}Q^{\mathbf{q}}_{a'l'm'}S^{aa'}_{(L+l')(M-m')}(\mathbf{k}) \tag{32c}$$

with the multipole moments

$$Q^{\mathbf{q}}_{alm} = 4\pi i^l \mathcal{I}_l(q,s_a)Y^*_{lm}(\mathbf{e}_\mathbf{q}) \tag{33}$$

and the integrals

$$\mathcal{I}_l(q,r) = \int_0^r r'^{l+2} j_l(qr')\, dr' \quad \text{and} \quad \mathcal{J}_{al}(q,r) = \int_r^{s_a} \frac{j_l(qr')}{r'^{l-1}}\, dr' \,, \tag{34}$$

for which analytic expressions are given in appendix B.

3.3. *IPW-IPW*

The remaining integrals

$$v_{\mathbf{G}\mathbf{G}'}(\mathbf{k}) = \iint \frac{M^{\mathbf{k}^*}_{\mathbf{G}}(\mathbf{r}) M^{\mathbf{k}}_{\mathbf{G}'}(\mathbf{r}')}{|\mathbf{r}-\mathbf{r}'|}\, d^3r\, d^3r' \tag{35}$$

are evaluated in a similar manner. The subtraction of the plane waves inside the MT spheres now leads to a decomposition of the matrix elements into four terms

$$v_{\mathbf{G}\mathbf{G}'}(\mathbf{k}) = v^{(\mathrm{a})}_{\mathbf{G}\mathbf{G}'}(\mathbf{k}) - v^{(\mathrm{b})}_{\mathbf{G}\mathbf{G}'}(\mathbf{k}) - v^{(\mathrm{c})}_{\mathbf{G}\mathbf{G}'}(\mathbf{k}) + v^{(\mathrm{d})}_{\mathbf{G}\mathbf{G}'}(\mathbf{k}) \,. \tag{36}$$

The first three can be calculated analytically and yield

$$v^{(\mathrm{a})}_{\mathbf{G}\mathbf{G}'}(\mathbf{k}) = \frac{1}{V}\int d^3r \int d^3r' \, \frac{e^{-i(\mathbf{k}+\mathbf{G})\cdot\mathbf{r}} e^{i(\mathbf{k}+\mathbf{G}')\cdot\mathbf{r}'}}{|\mathbf{r}-\mathbf{r}'|} = \delta_{\mathbf{G}\mathbf{G}'} \frac{4\pi}{|\mathbf{k}+\mathbf{G}|^2} \quad , \tag{37a}$$

$$v^{(\mathrm{b})}_{\mathbf{G}\mathbf{G}'}(\mathbf{k}) = \frac{1}{V}\int_{\mathrm{MT}} d^3r \int d^3r' \, \frac{e^{-i(\mathbf{k}+\mathbf{G})\cdot\mathbf{r}} e^{i(\mathbf{k}+\mathbf{G}')\cdot\mathbf{r}'}}{|\mathbf{r}-\mathbf{r}'|} = (\delta_{\mathbf{G}\mathbf{G}'} - \Theta_{\mathbf{G}-\mathbf{G}'}) \frac{4\pi}{|\mathbf{k}+\mathbf{G}'|^2} \quad , \tag{37b}$$

$$v^{(\mathrm{c})}_{\mathbf{G}\mathbf{G}'}(\mathbf{k}) = \frac{1}{V}\int d^3r \int_{\mathrm{MT}} d^3r' \, \frac{e^{-i(\mathbf{k}+\mathbf{G})\cdot\mathbf{r}} e^{i(\mathbf{k}+\mathbf{G}')\cdot\mathbf{r}'}}{|\mathbf{r}-\mathbf{r}'|} = (\delta_{\mathbf{G}\mathbf{G}'} - \Theta_{\mathbf{G}-\mathbf{G}'}) \frac{4\pi}{|\mathbf{k}+\mathbf{G}|^2} \quad , \tag{37c}$$

while we evaluate the fourth term

$$v^{(\mathrm{d})}_{\mathbf{G}\mathbf{G}'}(\mathbf{k}) = \frac{1}{V}\int_{\mathrm{MT}} d^3r \int_{\mathrm{MT}} d^3r' \, \frac{e^{-i(\mathbf{k}+\mathbf{G})\cdot\mathbf{r}} e^{i(\mathbf{k}+\mathbf{G}')\cdot\mathbf{r}'}}{|\mathbf{r}-\mathbf{r}'|} \tag{37d}$$

by again replacing the exponential functions with the Rayleigh expansion (13) and following the procedure outlined in Section 3.1 above. The subsequent summation over MT spheres and angular momenta yields

$$\begin{aligned} v^{(\mathrm{d})}_{\mathbf{G}\mathbf{G}'}(\mathbf{k}) = \frac{1}{\Omega}\Bigg(& \sum_a e^{i(\mathbf{G}'-\mathbf{G})\cdot\mathbf{R}_a} \sum_{l=0}^{l_{\mathrm{PW}}} \sum_m \frac{(4\pi)^3}{2l+1} Y_{lm}(\mathbf{e}_{\mathbf{q}}) Y^*_{lm}(\mathbf{e}_{\mathbf{q}'}) \mathcal{K}_{al}(q,q') \\ & + \sum_{l=0}^{l_{\mathrm{PW}}} \sum_{m=-l}^{l} \sum_{l'=0}^{l_{\mathrm{PW}}} \sum_{m'=-l}^{l} (-1)^{l'+m'} \sum_{a,a'} e^{-i\mathbf{q}\cdot\mathbf{R}_a} e^{i\mathbf{q}'\cdot\mathbf{R}_{a'}} c_{l'm',lm} Q^{\mathbf{q}*}_{alm} Q^{\mathbf{q}'}_{a'l'm'} S^{aa'}_{(l+l')(m-m')}(\mathbf{k}) \Bigg) \end{aligned} \tag{38}$$

with $\mathbf{q} = \mathbf{k} + \mathbf{G}$, $\mathbf{q}' = \mathbf{k} + \mathbf{G}'$ and the double integral

$$\mathcal{K}_{al}(q,q') = \int_0^{s_a}\int_0^{s_a} r^2 r'^2 j_l(qr) j_l(q'r') \frac{r^l_<}{r^{l+1}_>}\, dr\, dr' \,. \tag{39}$$

For the latter an analytic formula is derived in appendix B.

4. Expansion around $\mathbf{k} = \mathbf{0}$

Due to the long-range nature of the Coulomb interaction $v(r) = 1/r$ in real space, its Fourier transform $4\pi/k^2$ diverges for $\mathbf{k} \to \mathbf{0}$. As a consequence, the Coulomb matrix in the mixed product basis also diverges with a leading term proportional to $1/k^2$**.** Since the MT functions contain nontrivial $\mathbf{k}$-dependent coefficients,

we further have additional terms proportional to $1/k$. It is helpful to identify all relevant terms in advance. For this purpose we formally represent the basis functions by their Fourier transforms

$$M_I^{\mathbf{k}}(\mathbf{r}) = \frac{1}{\sqrt{V}} \sum_{\mathbf{G}} c_{I\mathbf{G}}(\mathbf{k}) e^{i(\mathbf{k}+\mathbf{G})\cdot\mathbf{r}} \tag{40}$$

with the coefficients

$$c_{I\mathbf{G}}(\mathbf{k}) = \frac{1}{\sqrt{V}} \int e^{-i(\mathbf{k}+\mathbf{G})\cdot\mathbf{r}} M_I^{\mathbf{k}}(\mathbf{r})\, d^3r\,. \tag{41}$$

The sum runs over all reciprocal lattice vectors $\mathbf{G}$. For the IPWs the coefficients are $\mathbf{k}$-independent and equal $c_{\mathbf{G}'\mathbf{G}}(\mathbf{k}) = \Theta_{\mathbf{G}-\mathbf{G}'}$ for $M_{\mathbf{G}'}^{\mathbf{k}}(\mathbf{r})$, but for the MT functions they exhibit a nontrivial $\mathbf{k}$ dependence. Using the expansion

$$M_I^{\mathbf{k}}(\mathbf{r}) \sim \frac{1}{\sqrt{V}} \sum_{\mathbf{G}} \left(c_{I\mathbf{G}} + \mathbf{k}\cdot\nabla c_{I\mathbf{G}} + \frac{1}{2}\mathbf{k}^{\mathrm{T}} \Delta c_{I\mathbf{G}} \mathbf{k} \right) e^{i(\mathbf{k}+\mathbf{G})\cdot\mathbf{r}} \tag{42}$$

for $\mathbf{k} \to \mathbf{0}$ with $c_{I\mathbf{G}} = c_{I\mathbf{G}}(\mathbf{k})|_{\mathbf{k}=\mathbf{0}}$, $\nabla c_{I\mathbf{G}} = \nabla_{\mathbf{k}} c_{I\mathbf{G}}(\mathbf{k})|_{\mathbf{k}=\mathbf{0}}$ and $\Delta c_{I\mathbf{G}} = \nabla_{\mathbf{k}} \nabla_{\mathbf{k}}^{\mathrm{T}} c_{I\mathbf{G}}(\mathbf{k})\big|_{\mathbf{k}=\mathbf{0}}$, we can write the Coulomb matrix elements in this limit as

$$\begin{aligned} v_{IJ}(\mathbf{k}) \sim\, & c_{I\mathbf{0}}^* c_{J\mathbf{0}} \frac{4\pi}{k^2} + \left[c_{I\mathbf{0}}^* (\mathbf{e}_{\mathbf{k}}\cdot\nabla c_{J\mathbf{0}}) + (\mathbf{e}_{\mathbf{k}}\cdot\nabla c_{I\mathbf{0}}^*) c_{J\mathbf{0}} \right] \frac{4\pi}{k} + \Big[(\mathbf{e}_{\mathbf{k}}\cdot\nabla c_{I\mathbf{0}}^*)\, (\mathbf{e}_{\mathbf{k}}\cdot\nabla c_{J\mathbf{0}}) \\ & + \frac{1}{2} c_{I\mathbf{0}}^* (\mathbf{e}_{\mathbf{k}}^{\mathrm{T}} \Delta c_{J\mathbf{0}} \mathbf{e}_{\mathbf{k}}) + \frac{1}{2} (\mathbf{e}_{\mathbf{k}}^{\mathrm{T}} \Delta c_{I\mathbf{0}}^* \mathbf{e}_{\mathbf{k}}) c_{J\mathbf{0}} \Big] 4\pi + \sum_{\mathbf{G}\neq\mathbf{0}} c_{I\mathbf{G}}^* c_{J\mathbf{G}} \frac{4\pi}{|\mathbf{G}|^2}\,. \end{aligned} \tag{43}$$

Evidently, all matrix elements contain divergent contributions proportional to $1/k^2$ in addition to a constant term. Furthermore, if $c_{I\mathbf{G}}(\mathbf{k})$ or $c_{J\mathbf{G}}(\mathbf{k})$ are truly $\mathbf{k}$-dependent, i.e., for matrix elements that involve MT functions, we also have terms proportional to $Y_{1m}^*(\mathbf{e}_{\mathbf{k}})/k$ and $Y_{2m}^*(\mathbf{e}_{\mathbf{k}})$ arising from the first and second square bracket, respectively (compare (A.5) and (A.8)). As a consequence, we can write

$$v_{IJ}(\mathbf{k}) \sim v_{IJ}^{(0)} + \sum_{l=0}^{2} \sum_{m=-l}^{l} v_{IJ,lm}^{(1)} \frac{Y_{lm}^*(\mathbf{e}_{\mathbf{k}})}{k^{2-l}}\,, \tag{44}$$

and from (15) follows

$$v_{JI}^{(0)} = v_{IJ}^{(0)*} \quad \text{and} \quad v_{JI,lm}^{(1)} = (-1)^m v_{IJ,l(-m)}^{(1)*}\,. \tag{45}$$

We will see in Section 4.4 below that the terms corresponding to $l > 0$ can in fact be eliminated if we perform a basis transformation to the set of eigenvectors of the Coulomb matrix. Nevertheless, for the sake of completeness we will here give the appropriate formulas for $v_{IJ,lm}^{(1)}$ with $l > 0$ in the original mixed product basis as well. As in the previous section, we proceed by discussing the blocks MT-MT, MT-IPW and IPW-IPW individually.

4.1. *MT-MT*

The second term on the right-hand side of (18), explicitly given in (26), diverges for $\mathbf{k} \to \mathbf{0}$ and $L + L' < 2$, because the leading term of $S_{lm}^{aa'}(\mathbf{k})$ is proportional to k^{2-l}, which is seen in the following way: For small $\mathbf{k}$ the sum over $\mathbf{T}$ in (27) is dominated by contributions belonging to large lattice vectors. Then one can approximate the sum by an integral

$$S_{lm}^{aa'}(\mathbf{k}) \sim e^{-i\mathbf{k}\cdot\mathbf{R}_{aa'}} \frac{1}{\Omega} \int \frac{e^{i\mathbf{k}\cdot\mathbf{T}}}{T^{l+1}} Y_{lm}^*(\mathbf{e}_{\mathbf{T}})\, d^3T = \frac{4\pi i^l}{(2l-1)!!\Omega} e^{-i\mathbf{k}\cdot\mathbf{R}_{aa'}} Y_{lm}^*(\mathbf{e}_{\mathbf{k}}) k^{l-2}\,, \tag{46}$$

where we have used (13), (B.2), and (A.4). The same expression appears in the first term of the reciprocal-space sum corresponding to $\mathbf{G} = \mathbf{0}$ in the Ewald summation. The remaining terms and the real-space sum yield an additional constant term $S_{lm}^{aa'}$, so that we obtain

$$S_{lm}^{aa'}(\mathbf{k}) \sim \frac{4\pi i^l}{(2l-1)!!\Omega} e^{-i\mathbf{k}\cdot\mathbf{R}_{aa'}} Y_{lm}^*(\mathbf{e}_{\mathbf{k}}) k^{l-2} + S_{lm}^{aa'} \tag{47}$$

for $l \leq 2$. After inserting this expansion into (26) we obtain

$$v^{(0)}_{aLMP,a'L'M'P'} = \delta_{aa'} v^{(\mathrm{a})}_{aLMP,a'L'M'P'} + (-1)^{L'+M'} c_{L'M',LM} Q_{a'L'P'} Q_{aLP} S^{aa'}_{(L+L')(M-M')}\,, \tag{48}$$

$$v^{(1)}_{aLMP,a'L'M'P';lm} = \delta_{l,L+L'}\delta_{m,M-M'}(-1)^{L'+M'} \frac{4\pi i^l}{(2l-1)!!\Omega} c_{L'M',LM} Q_{a'L'P'} Q_{aLP} \tag{49}$$

with $l \leq 2$.

4.2. *MT-IPW*

The case MT-IPW is more complicated, because higher orders in the multipole moments $Q^{\mathbf{k}+\mathbf{G}}_{a'l'm'}$ must be taken into account when multiplying with the divergent $S^{aa'}_{(L+l')(M-m')}(\mathbf{k})$ in (32c). In particular, we need the expansions of $Q^{\mathbf{k}+\mathbf{G}}_{a'00}$ ($Q^{\mathbf{k}+\mathbf{G}}_{a'1m'}$) up to second (first) order

$$Q^{\mathbf{k}+\mathbf{G}}_{a00} \sim \sqrt{4\pi}\frac{s_a^2}{G}\left[j_1(Gs_a) - j_2(Gs_a)s_a k\,\mathbf{e_k}\cdot\mathbf{e_G} + \frac{1}{2}j_3(Gs_a)s_a^2k^2\,(\mathbf{e_k}\cdot\mathbf{e_G})^2 - \frac{1}{2}\frac{j_2(Gs_a)}{G}s_a k^2\right], \tag{50a}$$

$$Q^{\mathbf{k}+\mathbf{G}}_{a1m} \sim 4\pi i\frac{s_a^3}{G}\left[Y^*_{1m}(\mathbf{e_G})\,(j_2(Gs_a) - j_3(Gs_a)s_a k\,\mathbf{e_k}\cdot\mathbf{e_G}) + Y^*_{1m}(\mathbf{e_k})\frac{j_2(Gs_a)}{G}k\right]. \tag{50b}$$

For $\mathbf{G} = \mathbf{0}$ these simplify to

$$Q^{\mathbf{k}}_{a00} \sim \frac{\sqrt{4\pi}}{3}s_a^3\left(1 - \frac{1}{10}s_a^2k^2\right), \tag{51a}$$

$$Q^{\mathbf{k}}_{a1m} \sim \frac{4\pi i}{15}Y^*_{1m}(\mathbf{e_k})s_a^5 k\,. \tag{51b}$$

Here we have used the identities (A.1)–(A.7). In addition, (32a) contributes to $v^{(1)}_{aLMP,\mathbf{G}}$ if $\mathbf{G} = \mathbf{0}$. The final expression for $v^{(0)}_{aLMP,\mathbf{G}}$ and $v^{(1)}_{aLMP,\mathbf{G}}$ is written as

$$v^{(0)}_{aLMP,\mathbf{G}} = v^{(0\mathrm{a})}_{aLMP,\mathbf{G}} + v^{(0\mathrm{b})}_{aLMP,\mathbf{G}}\,, \tag{52}$$

where the quantity

$$\begin{aligned} v^{(0\mathrm{a})}_{aLMP,\mathbf{G}} &= (1-\delta_{\mathbf{G0}})v^{(\mathrm{a})}_{aLMP,\mathbf{G}}(\mathbf{0}) + v^{(\mathrm{b})}_{aLMP,\mathbf{G}}(\mathbf{0}) \\ &\quad -\frac{1}{\sqrt{\Omega}}Q_{aLP}\sum_{l'=0}^{l_{\mathrm{PW}}}\sum_{m'=-l'}^{l'}(-1)^{l'+m'}\sum_{a'}e^{i\mathbf{G}\cdot\mathbf{R}_{a'}}c_{l'm',LM}Q^{\mathbf{G}}_{a'l'm'}S^{aa'}_{(L+l')(M-m')} \end{aligned} \tag{53}$$

is directly obtained after replacing $S^{aa'}_{lm}(\mathbf{k})$ by the terms of zeroth order in the expansion (47). The second term $v^{(0\mathrm{b})}_{aLMP,\mathbf{G}}$ results from multiplying the divergent terms in (47) with the higher orders of (50) in (32c) as well as, in the case $\mathbf{G} = \mathbf{0}$, the term $1/q^2$ with the higher orders of $j_l(qr)$ in (32a). After some algebra we obtain

$$v^{(0\mathrm{b})}_{aLMP,\mathbf{G}} = \begin{cases} -\dfrac{(4\pi)^{5/2}}{\Omega^{3/2}}Q_{a0P}\displaystyle\sum_{a'}e^{i\mathbf{G}\cdot\mathbf{R}_{a'}}\frac{s_{a'}^3}{G}\left[\frac{j_2(Gs_{a'})}{2G} - \frac{j_3(Gs_{a'})s_{a'}}{6}\right] & \text{if } \mathbf{G}\neq\mathbf{0} \text{ and } L=0\,, \\ -\dfrac{(4\pi)^{5/2}}{30\Omega^{3/2}}Q_{a0P}\displaystyle\sum_{a'}s_{a'}^5 + \frac{(4\pi)^{3/2}}{6\sqrt{\Omega}}\int_0^{s_a} r^4 M_{a0P}(r)dr & \text{if } \mathbf{G}=\mathbf{0} \text{ and } L=0\,, \\ -\dfrac{(4\pi)^{5/2}}{\Omega^{3/2}}Q_{a0P}\displaystyle\sum_{a'}e^{i\mathbf{G}\cdot\mathbf{R}_{a'}}\frac{s_{a'}^3}{G}\left[\frac{j_2(Gs_{a'})}{2G} - \frac{j_3(Gs_{a'})s_{a'}}{6}\right] & \text{if } \mathbf{G}\neq\mathbf{0} \text{ and } L=1\,, \\ 0 & \text{otherwise}\,, \end{cases} \tag{54}$$

as well as

$$v^{(1)}_{aLMP,\mathbf{G};lm} = \delta_{Ll}\delta_{Mm}\left[-\frac{(4\pi)^{5/2} i^L}{(2L+1)!!\Omega^{3/2}} Q_{aLP} \sum_{a'} e^{i\mathbf{G}\cdot\mathbf{R}_{a'}} Q^{\mathbf{G}}_{a'00} + \delta_{\mathbf{G0}} \frac{(4\pi)^2 i^L Q_{aLP}}{(2L+1)!!\Omega^{1/2}}\right] . \tag{55}$$

4.3. *IPW-IPW*

Finally, in the calculation of the IPW-IPW matrix elements we can use the fact that the square brackets in (43) vanish. This simplifies the derivation considerably, because all angular-dependent contributions can be discarded from the outset, and hence we have $v^{(1)}_{\mathbf{GG}',lm} = 0$ for $l > 0$. We again write

$$v^{(0)}_{\mathbf{GG}'} = v^{(0\mathrm{a})}_{\mathbf{GG}'} + v^{(0\mathrm{b})}_{\mathbf{GG}'} ,$$

where the first contribution $v^{(0\mathrm{a})}_{\mathbf{GG}'}$ is given by the nondivergent terms in (36) after replacing $S^{aa'}_{lm}(\mathbf{k})$ by $S^{aa'}_{lm}$, which yields

$$\begin{aligned} v^{(0\mathrm{a})}_{\mathbf{GG}'} &= (1-\delta_{\mathbf{G0}})\left[v^{(\mathrm{a})}_{\mathbf{GG}'}(\mathbf{0}) - v^{(\mathrm{c})}_{\mathbf{GG}'}(\mathbf{0})\right] - (1-\delta_{\mathbf{G}'\mathbf{0}}) v^{(\mathrm{b})}_{\mathbf{GG}'}(\mathbf{0}) \\ &+ \frac{1}{\Omega}\Bigg(\sum_a e^{i(\mathbf{G}'-\mathbf{G})\cdot\mathbf{R}_a} \sum_{l=0}^{l_{\mathrm{PW}}} \sum_m \frac{(4\pi)^3}{2l+1} Y_{lm}(\mathbf{e}_{\mathbf{G}}) Y^*_{lm}(\mathbf{e}_{\mathbf{G}'}) \mathcal{K}_{al}(q,q') \\ &\quad + \sum_{l=0}^{l_{\mathrm{PW}}} \sum_{m=-l}^{l} \sum_{l'=0}^{l_{\mathrm{PW}}} \sum_{m'=-l}^{l} (-1)^{l'+m'} \sum_{a,a'} e^{-i\mathbf{G}\cdot\mathbf{R}_a} e^{i\mathbf{G}'\cdot\mathbf{R}_{a'}} c_{l'm',lm} Q^{\mathbf{G}^*}_{alm} Q^{\mathbf{G}'}_{a'l'm'} S^{aa'}_{(l+l')(m-m')}\Bigg) . \end{aligned} \tag{56}$$

Further, by inserting the expansions (50) and (51) as well as the $\mathbf{k}$-dependent terms of (47) into (38) one obtains another constant contribution

$$v^{(0\mathrm{b})}_{\mathbf{GG}'} = \begin{cases} \dfrac{(4\pi)^3}{\Omega^2} \displaystyle\sum_{a,a'} e^{-i\mathbf{G}\cdot\mathbf{R}_a} e^{i\mathbf{G}'\cdot\mathbf{R}_{a'}} \frac{s_a^2 s_{a'}^2}{GG'} \Bigg\{ -\frac{1}{3} j_2(Gs_a) j_2(G's_{a'}) s_a s_{a'} (\mathbf{e}_{\mathbf{G}}\cdot\mathbf{e}_{\mathbf{G}'}) - \frac{1}{6} j_1(Gs_a) j_3(G's_{a'}) s_{a'}^2 \\ \quad -\frac{1}{6} j_3(Gs_a) j_1(G's_{a'}) s_a^2 + \frac{j_1(Gs_a) j_2(G's_{a'}) s_{a'}}{2G'} + \frac{j_2(Gs_a) j_1(G's_{a'}) s_a}{2G} \Bigg\} & \text{if } \mathbf{G}\neq\mathbf{0} \text{ and } \mathbf{G}'\neq\mathbf{0}, \\ \dfrac{(4\pi)^3}{\Omega^2} \displaystyle\sum_{a,a'} e^{i\mathbf{G}'\cdot\mathbf{R}_{a'}} \frac{s_a^3 s_{a'}^2}{G'} \left\{ \frac{s_a^2}{30} j_1(G's_{a'}) - \frac{1}{18} j_3(G's_{a'}) s_{a'}^2 + \frac{1}{6} \frac{j_2(G's_{a'})}{G'} s_{a'} \right\} & \text{if } \mathbf{G}=\mathbf{0} \text{ and } \mathbf{G}'\neq\mathbf{0}, \\ \dfrac{(4\pi)^3}{\Omega^2} \displaystyle\sum_{a,a'} e^{-i\mathbf{G}\cdot\mathbf{R}_{a'}} \frac{s_a^3 s_{a'}^2}{G} \left\{ \frac{s_a^2}{30} j_1(Gs_{a'}) - \frac{1}{18} j_3(Gs_{a'}) s_{a'}^2 + \frac{1}{6} \frac{j_2(Gs_{a'})}{G} s_{a'} \right\} & \text{if } \mathbf{G}\neq\mathbf{0} \text{ and } \mathbf{G}'=\mathbf{0}, \\ \dfrac{(4\pi)^3}{90\Omega^2} \displaystyle\sum_{a,a'} s_a^3 s_{a'}^3 \left(s_a^2 + s_{a'}^2\right) & \text{if } \mathbf{G}=\mathbf{G}'=\mathbf{0} . \end{cases} \tag{57}$$

For the calculation of $v^{(1)}_{\mathbf{GG}',00}$ we must take the divergent terms of (37) into account and eventually obtain

$$v^{(1)}_{\mathbf{GG}',00} = \frac{(4\pi)^{5/2}}{\Omega^2} \sum_{a,a'} e^{-i\mathbf{G}\cdot\mathbf{R}_a} e^{i\mathbf{G}'\cdot\mathbf{R}_{a'}} Q^{\mathbf{G}^*}_{a00} Q^{\mathbf{G}'}_{a'00} + (4\pi)^{3/2} \left[\Theta_{\mathbf{G}-\mathbf{G}'}(\delta_{\mathbf{G0}} + \delta_{\mathbf{G}'\mathbf{0}}) - \delta_{\mathbf{G0}}\delta_{\mathbf{G}'\mathbf{0}}\right] . \tag{58}$$

4.4. *Diagonalization*

In a pure plane-wave representation response matrices and similar quantities decompose into head $\chi_{\mathbf{00}}$, wings $\chi_{\mathbf{G0}}$, $\chi_{\mathbf{0G}'}$, and body $\chi_{\mathbf{GG}'}$ with $\mathbf{G},\mathbf{G}'\neq\mathbf{0}$. These behave differently for $\mathbf{k}\to\mathbf{0}$. For the density response function, as an example, head and wing elements are quadratic and linear in k, respectively, while the body elements remain finite but still exhibit an angular $\mathbf{k}$ dependence. As the mixed product basis is related to the set of plane waves by means of a basis transformation, these matrix elements will now mix in a complicated manner. It is hence desirable to make another transformation that restores the convenient

mathematical properties of the plane-wave basis. For this purpose the basis must include a constant function, which corresponds to the limit of $e^{i\mathbf{k}\cdot\mathbf{r}}/\sqrt{V}$ for $\mathbf{k}\to\mathbf{0}$ and is responsible for the decomposition into head, wings, and body. Such a basis is given by the functions

$$E_\mu^{\mathbf{k}}(\mathbf{r}) = \sum_I E_{\mu I}^{\mathbf{k}} M_I^{\mathbf{k}}(\mathbf{r})\,, \tag{59}$$

where $E_{\mu I}^{\mathbf{k}}$ is the Ith component of the μth eigenvector of $v_{IJ}(\mathbf{k})$. In this basis the Coulomb matrix $v_{\mu\nu}(\mathbf{k})$ becomes diagonal, which is also advantageous in matrix multiplications involving $v_{\mu\nu}(\mathbf{k})$, e.g., for the calculation of the dielectric function. Furthermore, the eigenvalues are a direct measure for the probability of the elastic scattering between two particles. Small eigenvalues thus identify less important scattering processes that might be neglected, leading to a smaller and optimized basis set after removal of the corresponding eigenvectors.

Because of the divergent terms in (44) the diagonalization in the limit $\mathbf{k}\to\mathbf{0}$ is not trivial. The first eigenvector $\mathbf{E}_1^{\mathbf{k}}$ corresponding to the divergent eigenvalue $v_1(\mathbf{k}) = 4\pi/k^2$ is, however, easy to obtain from the analytic projection of $e^{i\mathbf{k}\cdot\mathbf{r}}/\sqrt{V}$ on the biorthogonal mixed-product-basis functions

$$E_{1I}^{\mathbf{k}} = \frac{1}{\sqrt{V}}\int_V \tilde{M}_I^{\mathbf{k}^*}(\mathbf{r})\, e^{i\mathbf{k}\cdot\mathbf{r}}\, d^3r = \begin{cases} c_{I\mathbf{0}}^*(\mathbf{k}) = \dfrac{4\pi i^L}{\sqrt{\Omega}} Y_{LM}^*(\mathbf{e}_\mathbf{k}) \displaystyle\int_0^{s_a} r^2 j_L(kr) M_{aLP}(r)\, dr & \text{for } I = (aLMP)\,, \\ \delta_{\mathbf{G0}} & \text{for } I = \mathbf{G}\,, \end{cases} \tag{60}$$

which in the limit $\mathbf{k}\to\mathbf{0}$ becomes

$$E_{1I}^{\mathbf{0}} = \begin{cases} \sqrt{4\pi s_a^3/(3\Omega)} & \text{for } I = (a001)\,, \\ \delta_{\mathbf{G0}} & \text{for } I = \mathbf{G}\,, \\ 0 & \text{otherwise}\,. \end{cases} \tag{61}$$

Here we have assumed that the constant MT function of atom a is normalized and identified with the index $(a001)$. The other eigenvectors $\mathbf{E}_\mu^{\mathbf{0}}$ and eigenvalues $v_\mu(\mathbf{0})$ for $\mu > 1$ are obtained by diagonalizing the last term of the formal expansion (43)

$$\overline{v}_{IJ} = \sum_{\mathbf{G}\neq\mathbf{0}} c_{I\mathbf{G}}^* c_{J\mathbf{G}} \frac{4\pi}{G^2}\,, \tag{62}$$

which is unknown so far. The matrix $v_{IJ}^{(0)}$, calculated in the previous section, contains $\overline{v}_{IJ}$ but also the spherical average of the second square bracket in (43). If we denote this spherical average by w_{IJ}, then we can write

$$\overline{v}_{IJ} = v_{IJ}^{(0)} - w_{IJ}\,. \tag{63}$$

In order to evaluate w_{IJ} we introduce the natural basis

$$k_{-1} = \frac{1}{\sqrt{2}}(k_x - ik_y), \qquad k_1 = \frac{1}{\sqrt{2}}(-k_x - ik_y), \qquad k_0 = k_z\,, \tag{64a}$$

$$\partial_{-1} = \frac{1}{\sqrt{2}}(\partial_x + i\partial_y)\,, \quad \partial_1 = \frac{1}{\sqrt{2}}(-\partial_x + i\partial_y)\,, \quad \partial_0 = \partial_z\,, \tag{64b}$$

which allows us to write the $\mathbf{k}$-dependent terms in the second bracket of (43) in terms of spherical harmonics according to

$$\mathbf{e}_\mathbf{k}^\mathrm{T}\Delta c_{J\mathbf{0}}\mathbf{e}_\mathbf{k} = \frac{4\pi}{3}\sum_{m=-1}^{1}\sum_{m'=-1}^{1} Y_{1m}^*(\mathbf{e}_\mathbf{k})Y_{1m'}(\mathbf{e}_\mathbf{k})\partial_m^*\partial_{m'}c_{J\mathbf{0}} \tag{65}$$

$$= \frac{1}{3}\sum_{m=-1}^{1}\partial_m^*\partial_m c_{J\mathbf{0}} + \frac{4\pi}{3}\sum_{m=-1}^{1}\sum_{m'=-1}^{1} C_{1m'1m2(m-m')}Y_{2(m-m')}^*(\mathbf{e}_\mathbf{k})\partial_m^*\partial_{m'}c_{J\mathbf{0}}\,,$$

$$(\mathbf{e}_\mathbf{k}\cdot\nabla c_{I\mathbf{0}}^*)\,(\mathbf{e}_\mathbf{k}\cdot\nabla c_{J\mathbf{0}}) = \frac{4\pi}{3}\sum_{m=-1}^{1}\sum_{m'=-1}^{1} Y_{1m}^*(\mathbf{e}_\mathbf{k})Y_{1m'}(\mathbf{e}_\mathbf{k})\partial_m^* c_{I\mathbf{0}}^*\partial_{m'}c_{J\mathbf{0}} \tag{66}$$

$$= \frac{1}{3}\sum_{m=-1}^{1}\partial_m^* c_{I\mathbf{0}}^*\partial_m c_{J\mathbf{0}} + \frac{4\pi}{3}\sum_{m=-1}^{1}\sum_{m'=-1}^{1} C_{1m'1m2(m-m')}Y_{2(m-m')}^*(\mathbf{e}_\mathbf{k})\partial_m^* c_{I\mathbf{0}}^*\partial_{m'}c_{J\mathbf{0}}\,,$$

where we define $\partial_m c_{I\mathbf{0}} = \partial_m c_{I\mathbf{0}}(\mathbf{k})|_{\mathbf{k}=\mathbf{0}}$ and similar abbreviations. The last equation follows from the identity

$$\mathbf{e}_\mathbf{k}\cdot\nabla c_{I\mathbf{0}} = \sqrt{\frac{4\pi}{3}}\sum_{m=-1}^{1} Y_{1m}(\mathbf{e}_\mathbf{k})\partial_m c_{I\mathbf{0}}\,. \tag{67}$$

When we take the spherical average, the harmonics with $l > 0$ vanish, and we obtain

$$w_{IJ} = \frac{4\pi}{3}\sum_{m=-1}^{1}\left[(\partial_m^* c_{I\mathbf{0}}^*)\,(\partial_m c_{J\mathbf{0}}) + \frac{1}{2}c_{I\mathbf{0}}^*\partial_m^*\partial_m c_{J\mathbf{0}} + \frac{1}{2}c_{J\mathbf{0}}\partial_m\partial_m^* c_{I\mathbf{0}}^*\right] \tag{68}$$

with

$$c_{I\mathbf{0}} = \begin{cases} \sqrt{4\pi s_a^3/(3\Omega)} & \text{for } I = (a001)\,, \\ \Theta_{-\mathbf{G}} & \text{for } I = \mathbf{G}\,, \\ 0 & \text{otherwise}\,, \end{cases} \tag{69}$$

$$\partial_m c_{I\mathbf{0}} = \begin{cases} -\delta_{L1}\delta_{Mm}\sqrt{\dfrac{4\pi}{3\Omega}}\,i\displaystyle\int_0^{s_a} r^3 M_{a1P}(r)\,dr & \text{for } I = (a1MP)\,, \\ 0 & \text{otherwise}\,, \end{cases} \tag{70}$$

$$\sum_{m=-1}^{1}\partial_m\partial_m^* c_{I\mathbf{0}} = \begin{cases} -\delta_{L0}\sqrt{\dfrac{4\pi}{\Omega}}\displaystyle\int_0^{s_a} r^4 M_{a0P}(r)\,dr & \text{for } I = (a0MP)\,, \\ 0 & \text{otherwise}\,. \end{cases} \tag{71}$$

5. Test calculations

Apart from the evaluation of (27), which is easily converged to high precision by means of the Ewald summation technique, and the radial meshes for numerical integration inside the MT spheres, the cutoff value l_PW is the only convergence parameter in the construction of the Coulomb matrix elements presented above. On the other hand, in an alternative implementation that uses the representation (12) rather than the Rayleigh expansion for the IPWs the matrix elements must be converged with respect to the reciprocal cutoff radius G_PW. Figure 1 compares the convergence behavior of these two approaches. The curves indicate the root mean square deviation of the Coulomb matrix for bulk silicon, averaged over all matrix elements MT-IPW and IPW-IPW and over 64 $\mathbf{k}$ points, from the fully converged results calculated with $l_\mathrm{PW} = 26$. In both cases we employ the same cutoff parameters $G'_\mathrm{max} = 3.6\,\mathrm{Bohr}^{-1}$ and $L_\mathrm{max} = 4$ for the mixed product basis, the MT functions are constructed from products $u_{al0}^\sigma(r)u_{al'0}^\sigma(r)$ with $l \le 2$ and $l' \le 3$. On average this yields 411 basis functions per $\mathbf{k}$ point. It is evident that the results obtained with the present method converge much faster than those obtained with the Fourier transform of the step function. Furthermore, at the same level of accuracy the present method is typically by a factor of 10–100 faster.

As an application we now consider the simulation of experimental spectroscopies related to the complex dielectric function, which describes many-body screening effects in a correlated electron system. In electron-energy-loss spectroscopy (EELS), for example, the measured differential scattering cross section is directly proportional to the imaginary part of a diagonal element of the inverse dielectric function [19]

$$\varepsilon^{-1}(\mathbf{k},\omega) = \frac{1}{V}\iint \varepsilon^{-1}(\mathbf{r},\mathbf{r}';\omega)e^{i\mathbf{k}\cdot(\mathbf{r}'-\mathbf{r})}d^3r\,d^3r'\,, \tag{72}$$

whereas in optical absorption one measures the imaginary part of [20]

$$\varepsilon_{\mathrm{M}}(\omega) = \lim_{\mathbf{k}\to\mathbf{0}} 1/\varepsilon^{-1}_{\mathrm{M}}(\mathbf{k},\omega)\,. \tag{73}$$

In the framework of many-body perturbation theory the dielectric function is written as

$$\varepsilon(\mathbf{r},\mathbf{r}';\omega) = \delta(\mathbf{r}-\mathbf{r}') - \int v(\mathbf{r},\mathbf{r}'')P(\mathbf{r}'',\mathbf{r}';\omega)\,d^3r'' \tag{74}$$

with the polarization function $P(\mathbf{r},\mathbf{r}';\omega)$ and the Coulomb interaction $v(\mathbf{r},\mathbf{r}') = 1/|\mathbf{r}-\mathbf{r}'|$. We use the random-phase approximation

$$\begin{aligned} P(\mathbf{r},\mathbf{r}';\omega) = \sum_{\sigma}\sum_{n,\mathbf{q}}^{\mathrm{occ}}\sum_{n',\mathbf{k}}^{\mathrm{unocc}} & \varphi^{\sigma *}_{n\mathbf{k}}(\mathbf{r})\varphi^{\sigma}_{n'\mathbf{q}+\mathbf{k}}(\mathbf{r})\varphi^{\sigma}_{n\mathbf{k}}(\mathbf{r}')\varphi^{\sigma *}_{n'\mathbf{q}+\mathbf{k}}(\mathbf{r}') \\ & \times\left(\frac{1}{\omega+\epsilon^{\sigma}_{n\mathbf{k}}-\epsilon^{\sigma}_{n'\mathbf{q}+\mathbf{k}}+i\eta} - \frac{1}{\omega-\epsilon^{\sigma}_{n\mathbf{k}}+\epsilon^{\sigma}_{n'\mathbf{q}+\mathbf{k}}-i\eta}\right)\,, \end{aligned} \tag{75}$$

where η is a positive infinitesimal. As $P(\mathbf{r},\mathbf{r}';\omega)$ contains products of wave functions evaluated at $\mathbf{r}$ and $\mathbf{r}'$, it can be represented in the mixed product basis as

$$P(\mathbf{r},\mathbf{r}';\omega) = \sum_{I,J}\int_{\mathrm{BZ}} P_{IJ}(\mathbf{k},\omega)M^{\mathbf{k}}_I(\mathbf{r})M^{\mathbf{k}^*}_J(\mathbf{r}')\,d^3k \tag{76}$$

with complex coefficients

$$P_{IJ}(\mathbf{k},\omega) = \iint P(\mathbf{r},\mathbf{r}';\omega)\tilde{M}^{\mathbf{k}^*}_I(\mathbf{r})\tilde{M}^{\mathbf{k}}_J(\mathbf{r}')\,d^3r\,d^3r'\,. \tag{77}$$

Next we transform this matrix to the basis given by (59). This yields $P_{\mu\nu}(\mathbf{k},\omega)$, which in the limit $\mathbf{k}\to\mathbf{0}$ decomposes into head, wing, and body elements as discussed in Section 4.4. We use the tetrahedron method for integrations over the BZ.

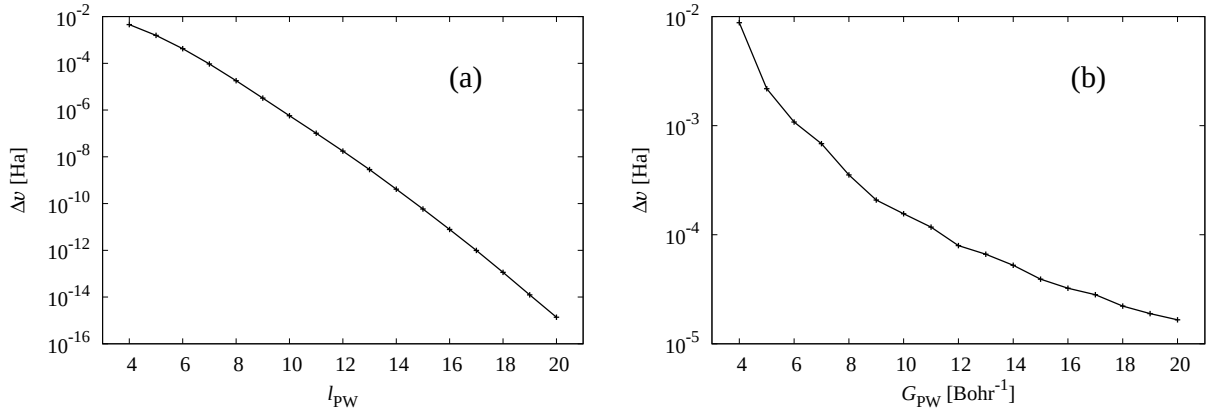

Figure 1. Average root mean square deviation Δv from the converged matrix elements (MT-IPW and IPW-IPW) as functions of (a) the convergence parameters l_{PW} and (b) the reciprocal cutoff radius G_{PW} for the Fourier transform of the step function in (12). The mixed product basis was optimized for Si bulk.

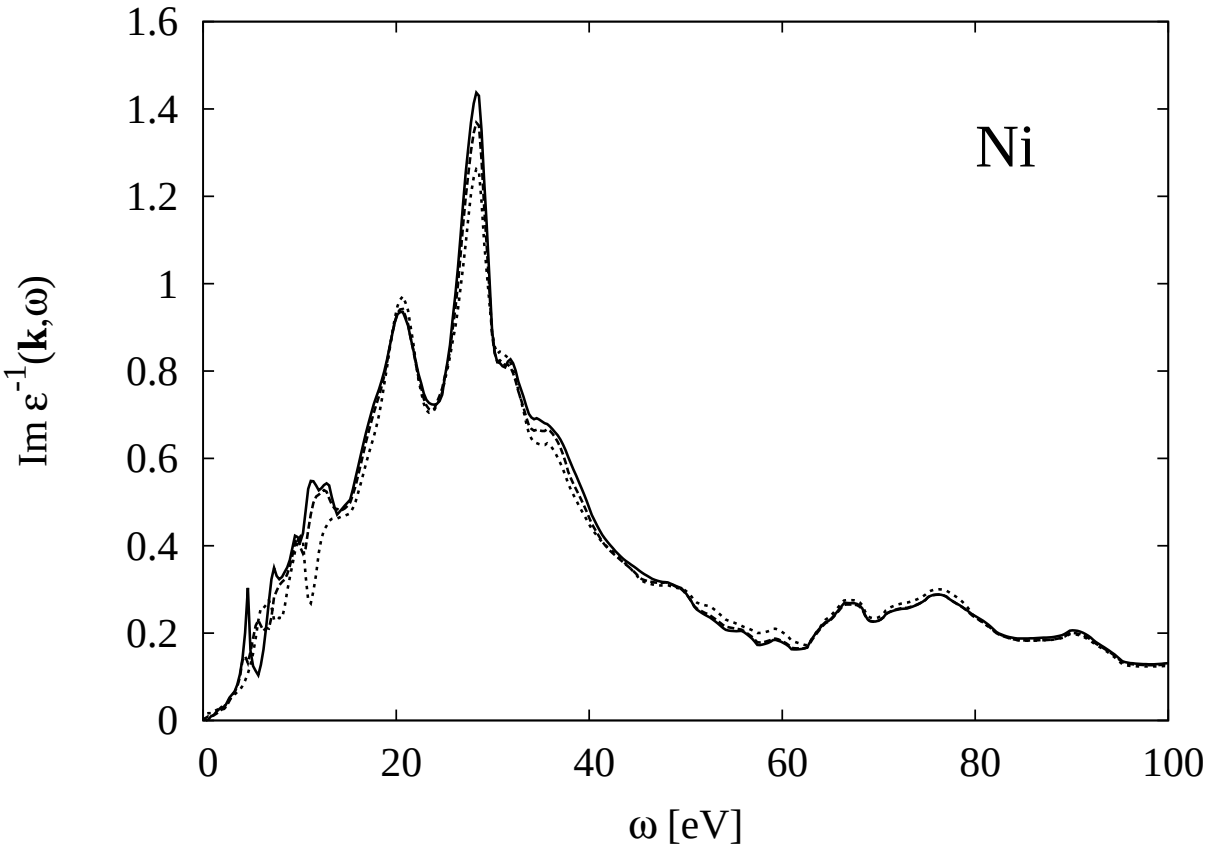

Figure 2. EELS spectra of spin-polarized Ni for $\mathbf{k} = 2\pi/a_{\mathrm{Ni}}(\xi,\xi,\xi)$ with $\xi = 0$ (solid line), $\xi = 0.1$ (dashed line), and $\xi = 0.2$ (dotted line).

In the long-wave-length limit $\mathbf{k} \to \mathbf{0}$ we must carefully expand the polarization function around $\mathbf{k} = \mathbf{0}$, since it is multiplied with $v(\mathbf{r},\mathbf{r}')$ in (74), which diverges in this limit. Because of the orthogonality of the wave functions the projection $\langle E_1^{\mathbf{k}}\varphi^\sigma_{n\mathbf{q}}|\varphi^\sigma_{n'\mathbf{q}+\mathbf{k}}\rangle = \langle e^{i\mathbf{k}\cdot\mathbf{r}}\varphi^\sigma_{n\mathbf{q}}|\varphi^\sigma_{n'\mathbf{q}+\mathbf{k}}\rangle/\sqrt{V}$ is linear in lowest order in $\mathbf{k}$ for interband transitions with $n \neq n'$. We calculate this leading term with $\mathbf{k}\cdot\mathbf{p}$ perturbation theory [21]. For a metallic system the sum in (75) also contains contributions from intraband transitions with $n = n'$ at $\mathbf{k} = \mathbf{0}$. It can be shown that these are nonzero only for the head element and given analytically by the Drude formula [22], which is quadratic in $\mathbf{k}$. The latter depends on the plasma frequency, which we obtain by an integration over the Fermi surface. In conclusion, the head and wing elements of $P_{\mu\nu}(\mathbf{k},\omega)$ are quadratic and linear in $\mathbf{k}$, respectively. If we use the symmetrized dielectric matrix

$$\tilde{\varepsilon}_{\mu\nu}(\mathbf{k},\omega) = \delta_{\mu\nu} - v_\mu^{1/2}(\mathbf{k}) P_{\mu\nu}(\mathbf{k},\omega) v_\nu^{1/2}(\mathbf{k})\,, \tag{78}$$

where the $v_\mu(\mathbf{k})$ are the eigenvalues of $v_{IJ}(\mathbf{k})$, then all elements of $\tilde{\varepsilon}_{\mu\nu}(\mathbf{k},\omega)$ are finite because $v_1^{1/2}(\mathbf{k}) = \sqrt{4\pi}/k$. We note that the diagonal quantities considered above remain unchanged with this symmetrized definition. As the first eigenvector of $v_{IJ}(\mathbf{k})$ corresponds to the projection of $e^{i\mathbf{k}\cdot\mathbf{r}}/\sqrt{V}$ onto the biorthogonal mixed product basis, the head element $\tilde{\varepsilon}^{-1}_{11}(\mathbf{k},\omega)$ directly equals the spectroscopic function (72).

In figure 2 we show EELS spectra $\mathrm{Im}\,\varepsilon^{-1}(\mathbf{k},\omega)$ for spin-polarized Ni at three $\mathbf{k}$ vectors $2\pi/a_{\mathrm{Ni}}(\xi,\xi,\xi)$ with $\xi = 0.0,\ 0.1,\ 0.2$ and the lattice constant $a_{\mathrm{Ni}} = 6.66\,\mathrm{Bohr}$ We use the parameters $l_{\max} = 8$, $G_{\max} = 3.57\,\mathrm{Bohr}^{-1}$ for the FLAPW and $L_{\max} = 4$, $G_{\max} = 5.00\,\mathrm{Bohr}^{-1}$ for the mixed product basis. The BZ is sampled by 1661 points in its irreducible wedge, corresponding to a $40\times40\times40$ $\mathbf{k}$-point mesh in the full zone. As the spectrum extends over a wide energy range up to 100 eV, we augment the FLAPW basis by second and third energy derivatives as local orbitals to guarantee an accurate description of high-lying conduction

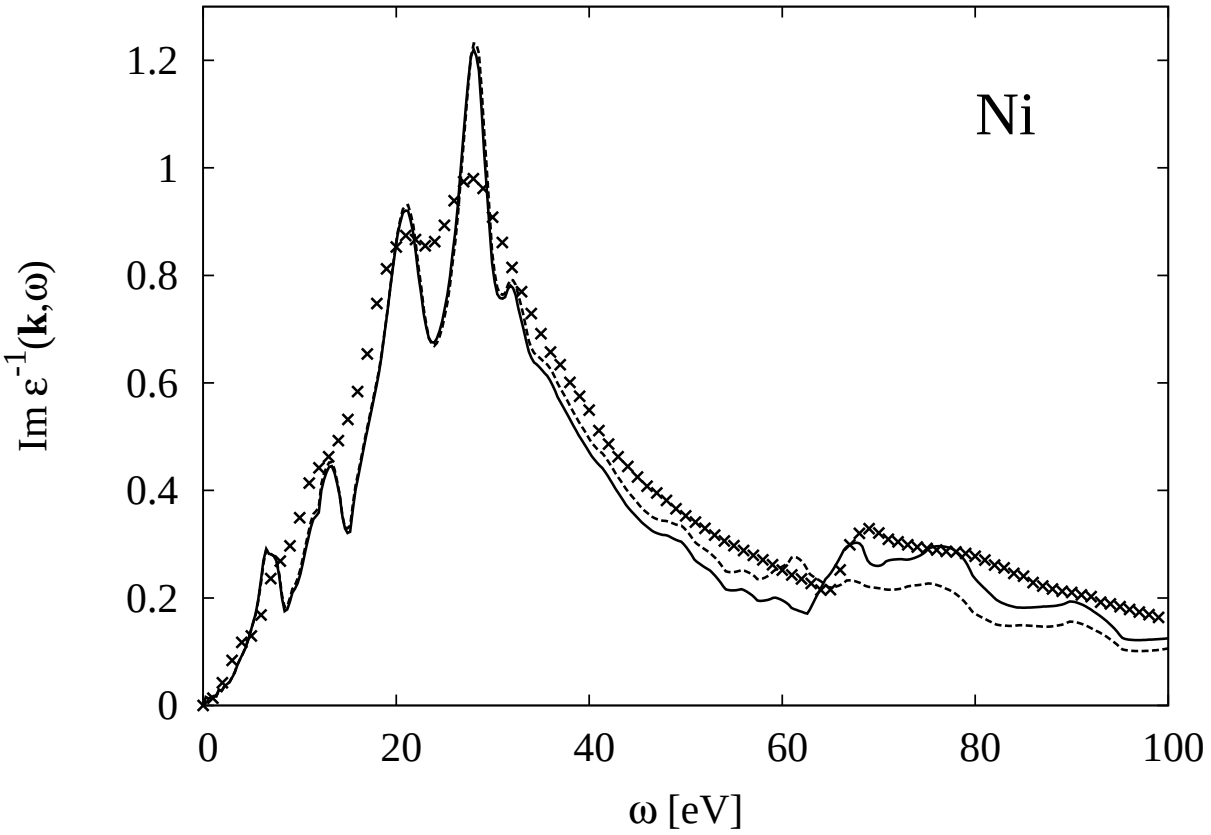

Figure 3. EELS spectra of spin-polarized Ni for $\mathbf{k} = 2\pi/a_{\mathrm{Ni}}(0.25, 0, 0)$ with (solid line) and without (dashed line) core-state contributions. The inclusion of transitions from core into conduction states gives rise to a shallow peak starting at 62 eV, which is also seen in experiment (symbols) [23].

states [15]. For the construction of the MT functions $M_{aLP}(r)$ we employ products $u^{\sigma}_{alp}(r)u^{\sigma}_{al'p}(r)$ with $l \leq 2$, $l' \leq 3$, and $p = 0$, i.e., energy derivatives ($p \geq 1$) are neglected. In the calculation of (75) we take 118 conduction and the 10 valence states as well as the eight $3s$ and $3p$ core states into account. As we invert the dielectric function, local-field effects are fully included. As seen from the figure, the spectra are very similar for the three $\mathbf{k}$ vectors. When compared with the curves calculated at finite $\mathbf{k}$ points, the spectrum for $\mathbf{k} = \mathbf{0}$ clearly constitutes the limit $\mathbf{k} \to \mathbf{0}$.

As already pointed out, the spectra in figure 2 already include transitions from the $3s$ and $3p$ core states into conduction states. Figure 3 shows a comparison of spectra calculated with (solid line) and without (dashed line) these core-state contributions at $\mathbf{k} = 2\pi/a_{\mathrm{Ni}}(0.25, 0, 0)$. The largest difference between the two curves is seen around 62 eV, which corresponds roughly to the threshold energy required to excite a $3p$ electron above the Fermi level. These additional transitions give rise to a shallow peak, which is also observed in experiments with an onset at the same energy. The inclusion of transitions from $3s$ and $3p$ core states into conduction states within our all-electron method thus brings the calculated spectrum very close to experiment (symbols) [23].

6. Summary

In this work we have derived formulas for the Coulomb matrix elements within the all-electron FLAPW method. As the Coulomb interaction couples two incoming and two outgoing states, a suitable basis set must be capable of accurately represent wave-function products. Such a set is given by the mixed product

basis, which contains MT functions as well as interstitial plane waves. We use the Rayleigh expansion for the latter, because it makes a very efficient numerical implementation possible. Furthermore, we have derived an exact expansion of the Coulomb matrix around $\mathbf{k} = \mathbf{0}$ that isolates all divergent terms $\sim k^{-2}$ and $\sim k^{-1}$. Most of these vanish if we then make a basis transformation to the eigenvectors of the Coulomb matrix. The properties of this new basis set are formally similar to those of a plane-wave basis. In particular, response functions decompose into head, wing, and body elements with the same characteristic dependence on $\mathbf{k}$. However, the basis construction of this involves no approximation, and the accuracy of the FLAPW basis set is completely preserved.

As an illustration we have shown EELS spectra for ferromagnetic Ni at different $\mathbf{k}$ vectors including $\mathbf{k} = \mathbf{0}$. Very good agreement with experiment was achieved over a large energy window by taking core-electron contributions into account.

Acknowledgements We gratefully acknowledge financial support from the Deutsche Forschungsgemeinschaft through the Priority Program 1145.

Appendix A. Mathematical relations

In the derivations of Sections 3 and 4 we have used the following relations:

$$j_{l-1}(x) + j_{l+1}(x) = (2l+1) j_l(x)/x \,, \tag{A.1}$$

$$\frac{d}{dx} j_l(x) = \frac{l}{x} j_l(x) - j_{l+1}(x) \,, \tag{A.2}$$

$$\frac{d}{dx} j_l(x) = j_{l-1}(x) - \frac{l+1}{x} j_l(x) \,, \tag{A.3}$$

$$j_l(x) = \frac{x^l}{(2l+1)!!} \left(1 - \frac{x^2}{4l+6} + \mathrm{O}(x^4) \right) \,, \tag{A.4}$$

$$\mathbf{e_k} \cdot \mathbf{e_G} = \frac{4\pi}{3} \sum_{m=-1}^{1} Y_{1m}(\mathbf{e_k}) Y^*_{1m}(\mathbf{e_G}), \tag{A.5}$$

$$Y_{1m}(\mathbf{e_a}) Y^*_{1m'}(\mathbf{e_a}) = \frac{1}{4\pi} \delta_{mm'} + C_{1m1m'2(m'-m)} Y^*_{2,m'-m}(\mathbf{e_a}) \,, \tag{A.6}$$

$$Y^*_{1m}(\mathbf{e_{k+G}}) = Y^*_{1m}(\mathbf{e_G}) + \frac{2k}{3G} \left[Y^*_{1m}(\mathbf{e_k}) - 2\pi \sum_{m'=-1}^{1} C_{m'm} Y^*_{2,m-m'}(\mathbf{e_G}) Y^*_{1m'}(\mathbf{e_k}) \right] + \mathrm{O}(k^2) \tag{A.7}$$

$$(\mathbf{e_k} \cdot \mathbf{e_G})^2 = \frac{1}{3} + \frac{8\pi}{15} \sum_{m'=-2}^{2} Y^*_{2m'}(\mathbf{e_k}) Y_{2m'}(\mathbf{e_G}) \,, \tag{A.8}$$

$$Y_{1m}(\mathbf{e_k}) = \sqrt{\frac{3}{4\pi}} \frac{k_m}{k} \,, \tag{A.9}$$

$$\sum_{m=-1}^{1} \partial_m \partial^*_m f(k) Y_{lm}(\mathbf{e_k}) = \frac{1}{k^2} Y_{lm}(\mathbf{e_k}) \left[\partial_k \left(k^2 \partial_k \right) - l(l+1) \right] f(k) \,. \tag{A.10}$$

Appendix B. Integrals over spherical Bessel functions

The derivations in Section 3 give rise to a number of integrals over spherical Bessel functions that can be evaluated analytically. Explicit formulas for (34) follow from the recursion relations (A.1)-(A.3)

$$\mathcal{I}_l(q,r) = \begin{cases} \dfrac{r^{l+2}}{q} j_{l+1}(qr) & \text{if } q \neq 0\,, \\ \delta_{l0}\dfrac{1}{3}r^3 & \text{if } q = 0\,, \end{cases} \tag{B.1}$$

$$\mathcal{J}_{al}(q,r) = \begin{cases} \dfrac{1}{q}\left[\dfrac{1}{r^{l-1}} j_{l-1}(qr) - \dfrac{1}{s_a^{l-1}} j_{l-1}(qs_a)\right] & \text{if } q \neq 0\,, \\ \delta_{l0}\dfrac{1}{2}\left(s_a^2 - r^2\right) & \text{if } q = 0\,. \end{cases} \tag{B.2}$$

We can also find an analytic expression for the double integral (39), because the above integration formulas and the recursion relation (A.1) lead to the solution

$$\begin{aligned} \mathcal{K}_{al}(q,q') &= \frac{2l+1}{q'^2}\int_0^{s_a} r^2 j_l(qr) j_l(q'r)\, dr - \frac{s_a^3}{qq'} j_{l+1}(qs_a) j_{l-1}(q's_a) \\ &= \frac{s_a^3}{q^2 - q'^2}\left[\frac{q'}{q} j_{l+1}(qs_a) j_{l-1}(q's_a) - \frac{q}{q'} j_{l-1}(qs_a) j_{l+1}(q's_a)\right] \qquad \text{(B.3a)} \\ &= s_a^3\left[\frac{j_{l+1}(qs_a) j_{l+1}(q's_a)}{qq'} + \frac{2l+1}{2l+3}\frac{j_{l+2}(qs_a) j_l(q's_a) - j_l(qs_a) j_{l+2}(q's_a)}{q^2 - q'^2}\right], \qquad \text{(B.3b)} \end{aligned}$$

where we used the symmetry of $\mathcal{K}_{al}(q,q')$ with respect to q and q' to eliminate $\int_0^{s_a} r^2 j_l(qr) j_l(q'r) dr$. The expressions (B.3a) and (B.3b) are stable for large and small q, q', respectively. The limiting cases are

$$\lim_{q'\to 0} \mathcal{K}_{al}(q,q') = \delta_{l0}\frac{s_a^3}{3q^2}\left[qs_a j_1(qs_a) + j_2(qs_a)\right] \quad \text{for } q \neq 0 \quad , \tag{B.4a}$$

$$\lim_{q'\to q} \mathcal{K}_{al}(q,q') = \frac{s_a^3}{2q^2}\left[(2l+3) j_{l+1}^2(qs_a) - (2l+1) j_l(qs_a) j_{l+2}(qs_a)\right] \quad \text{for } q \neq 0 \quad , \tag{B.4b}$$

$$\lim_{q,q'\to 0} \mathcal{K}_{al}(q,q') = \delta_{l0}\frac{2}{15} s_a^5 \quad . \tag{B.4c}$$

References

[1] P. Hohenberg, W. Kohn, Phys. Rev. 136 (1964) B864; W. Kohn, L.J. Sham, Phys. Rev. 140 (1965) A1133.
[2] G.D. Mahan, Many-Particle Physics, Plenum, New York, 1990.
[3] L. Hedin, Phys. Rev. 139 (1965) A796.
[4] W.G. Aulbur, L. Jönsson, J.W. Wilkins, in: H. Ehrenreich, F. Spaepen (Eds.) Solid State Physics, Vol. 54, Academic, San Diego, 2000, p. 1 and references therein.
[5] S. Albrecht, L. Reining, R. Del Sole, G. Onida, Phys. Rev. Lett. 80 (1998) 4510; L.X. Benedict, E.L. Shirley, R.B. Bohn, Phys. Rev. Lett. 80 (1998) 4514; M. Rohlfing, S.G. Louie, Phys. Rev. Lett. 81 (1998) 2312.
[6] V. Olevano, L. Reining, Phys. Rev. Lett. 86 (2001) 5962.
[7] D.J. Singh, Planewaves, Pseudopotentials and the LAPW Method, Kluwer, Dordrecht, 1994.
[8] T. Kotani, M. van Schilfgaarde, Solid State Commun. 121 (2002) 461.
[9] W. Ku, A.G. Eguiluz, Phys. Rev. Lett. 89 (2002) 126401.
[10] P. Puschnig, C. Ambrosch-Draxl, Phys. Rev. B 66 (2002) 165105.
[11] S. Lebègue, B. Arnaud, M. Alouani, P.E. Bloechl, Phys. Rev. B 67 (2003) 155208.
[12] C. Friedrich, A. Schindlmayr, S. Blügel (unpublished); http://www.flapw.de/spex.
[13] F. Aryasetiawan, O. Gunnarsson, Phys. Rev. B 49 (1994) 16214.
[14] D. Singh, Phys. Rev. B 43 (1991) 6388.
[15] C. Friedrich, A. Schindlmayr, S. Blügel, T. Kotani, Phys. Rev. B 74 (2006) 045104.
[16] A. Svane, O.K. Andersen, Phys. Rev. B 34 (1986) 5512.
[17] H.L. Skriver, The LMTO Method, Springer, Berlin, 1984.
[18] J.D. Talman, Special Functions, W.A. Benjamin, New York, 1968.
[19] G. Onida, L. Reining, A. Rubio, Rev. Mod. Phys. 74 (2002) 601.
[20] S.L. Adler, Phys. Rev. 126 (1962) 413; N. Wiser, Phys. Rev. 129 (1963) 62.
[21] S. Baroni, R. Resta, Phys. Rev. B 33 (1986) 7017.
[22] P. Ziesche, G. Lehmann (Eds.), Ergebnisse in der Elektronentheorie der Metalle, Akademie/Springer, Berlin, 1983.
[23] L.A. Feldkamp, M.B. Stearns, S.S. Shinozaki, Phys. Rev. B 20 (1979) 1310.